Simulation Study of Scintillator-based Calorimeter

H. Matsunaga, A. Nagano, S. Yamauchi, S. Kim
University of Tsukuba, Tsukuba, Ibaraki 305-8571, Japan
M. C. Chang
Tohoku University, Sendai, Miyagi 980-8578, Japan

Scintillator-based calorimeter is considered as a good choice for the linear collider for its design flexibility and inexpensive cost. To achieve fine granularity with the scintillator, we proposed using strip scintillators and evaluated the performance of the test module with beams. In this article, we compare the testbeam results with simulations, especially for the lateral shower spreads which are important for measuring jet energies. In addition, preliminary studies of GEANT4 with the simple sampling configuration are described.

1. INTRODUCTION

Excellent jet energy resolution is required for the future linear collider experiments where many jets are produced in the final states. Since tracking detectors can measure the particle momentum better than calorimeter, calorimeter should have good capability to separate neutral particles from charged particles and to measure accurately energies only from the neutrals. To make such measurements, granularity is more important than the energy resolution for single particles in designing the calorimeter.

Scintillator-based calorimeter has advantages of the design flexibility for the granularity, good timing resolution and hermeticity, and can be constructed with reasonable cost. In addition, excellent energy resolution and linearity for single particles can be achieved with the hardware compensation [1]. To achieve the excellent granularity, we have been studying the EM calorimeter using scintillator-strip arrays sandwiched between lead plates [2], which should provide effectively fine granularity of the strip-width. We compare testbeam results with simulation ones, and verify the potential ability to separate clusters.

We still need to examine the jet energy resolution with the full detector. As a first step of the simulation study, we check the fundamental behaviors of the sampling calorimeter using thin scintillator within the GEANT4 framework, and compare with the testbeam results of the energy resolution for the single particles.

2. STRIP-SCINTILLATOR EM CALORIMETER

2.1. Testbeams

To verify the performance of the scintillator-strip calorimeter with testbeams, we constructed a EM calorimeter test module (Figure 1). It consists of 24 layers (17 X_0) with a cross section of 20 cm $\times$ 20 cm. Each layer has a 4 mm-thick lead plates and two orthogonal scintillator-strip arrays. The size of a strip is 20 cm $\times$ 1cm-width $\times$ 2 mm-think, and the effective granularity becomes 1 cm $\times$ 1cm with the two orthogonal arrays. The length and the width of the strip, however, are not yet optimized, and the capability to detect multi-hits is also to be studied with the simulation. A 1 mm-ϕ WLS fiber is embedded into a straight groove of the strip. A clear fiber is connected to the WLS fiber outside the module, and goes to a 16-ch multi-anode PMT in the beam test. The consecutive four layers are ganged as one superlayer at a channel of the PMT.

We performed two beam tests in 2002 and 2004 at $\pi 2$ beamline of the KEK-PS. The beam contains pions, muons, electrons and protons in the energy region 1 $-$ 4 GeV. Trigger counters made of plastic scintillators are used to make an inclusive trigger, and two gas Čerenkov counters are placed on the beamline for the electron identification. Four

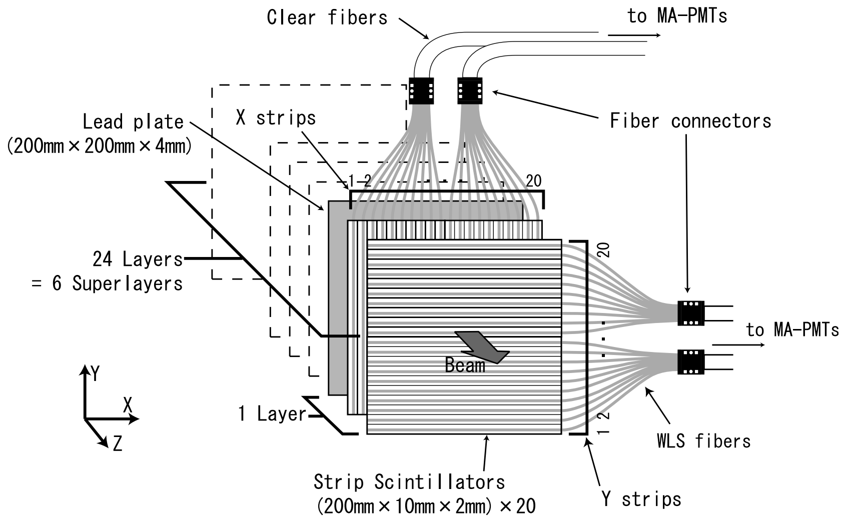

Figure 1: EM calorimeter test module.

single-wire drift chambers, each of which has a sense wire in each of two dimensions perpendicular to the beam incident direction, are utilized for the track reconstruction of the incident particle.

2.2. Energy Measurements

The energy resolution and linearity are measured with the electron beams. Figure 2(a) shows the results of the energy resolution measured by the x- or y-strips, or the all strips. The obtained resolution for all strips is $13.1\%/\sqrt{E} + 0.1\%$, where E is in GeV. The results are well reproduced by the MC simulation.

Figure 2(b) shows the linearity of the energy measurements for the real data and the simulation. The absolute

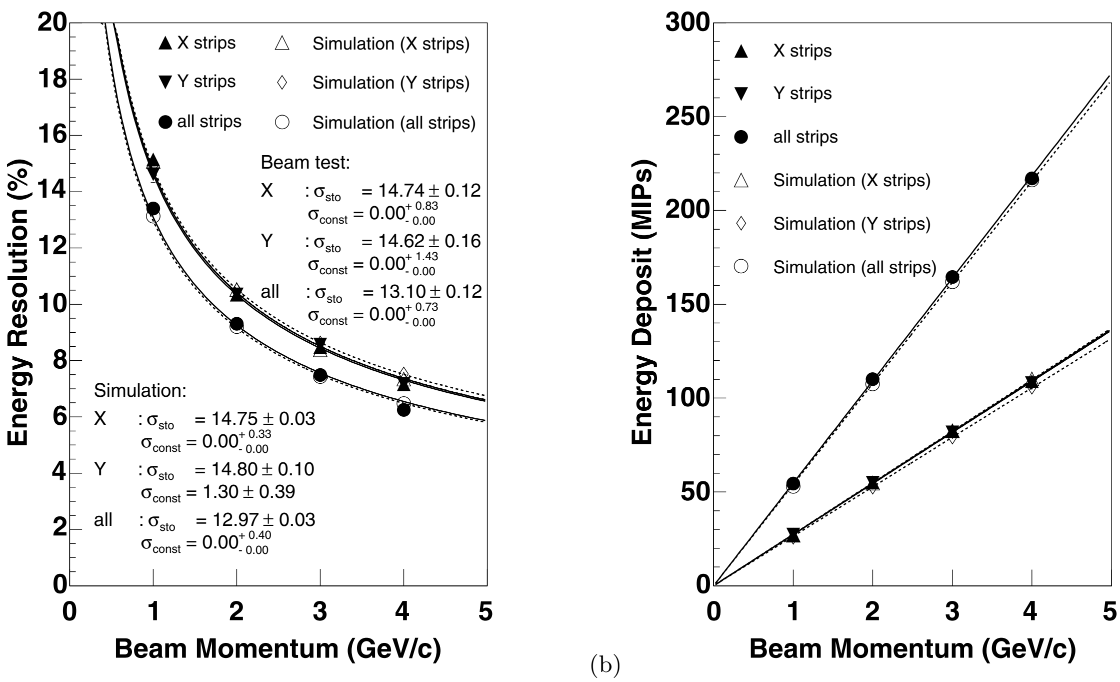

(a) (b)

Figure 2: (a) Energy resolution and (b) linearly as a function of incident beam momentum.

measured energies, in unit of the deposited energy for minimum ionizing particles (MIPs), agree well with the simulation results, after correcting detector effects such as light leakage between adjacent strips or cross-talks in the multi-anode PMTs. The deviations from the linearity are less than 1% for 2–4 GeV, and less than 2 % for 1 GeV where effect from materials in front of the test module becomes larger.

2.3. Lateral Shower Profiles

In order to examine the lateral shower spread, we introduce the energy fraction $I(x)$, which is defined as the energy deposit integrated between minus infinity and x, divided by the total energy deposit:

$$I(x) = \int_{-\infty}^{x} \rho(x')dx' \Big/ \int_{-\infty}^{\infty} \rho(x')dx'$$

where ρ represents the shower density. The origin of x is set, event by event, to the particle incident position determined by the extrapolation of the reconstructed track, hence $I(0) = 0.5$ with this definition.

Figure 3(a) shows the $I(x)$ for the x-strips of all superlayers for 4 GeV electrons and of the 2nd superlayer for MIPs. Note that in this figure we plot $I(x)$ as a sum of $I(-x)$ and $1 - I(x)$. The MIP spreads mainly originates from light leakage strips and cross-talks. On the other hand, the spreads for electrons mostly come from the EM shower spread in the calorimeter. To see the contributions to the spreads, we perform a simulation without the detector effects mentioned above, and compare the results with the data, as shown in Fig. 3(b). The simulation gives smaller spreads than the real data. We then make a smeared function as a convolution of the fitting results of the MIP and the simulation points. The obtained function, shown as dashed curve in Fig. 3(b), is consistent with the beam data.

Figure 4 shows the root-mean-square of hit clusters in each superlayer for 4 GeV electron events. This shows the fluctuation of the lateral profile of the EM shower. Taking account of the detector effects, the simulation gives almost same distributions as the real data.

These results concerning the lateral shower profiles are consistent with the expectation from the segmentation and the effective Molière radius (27 mm), and seem to be good at the basic level for the linear collider calorimeter.

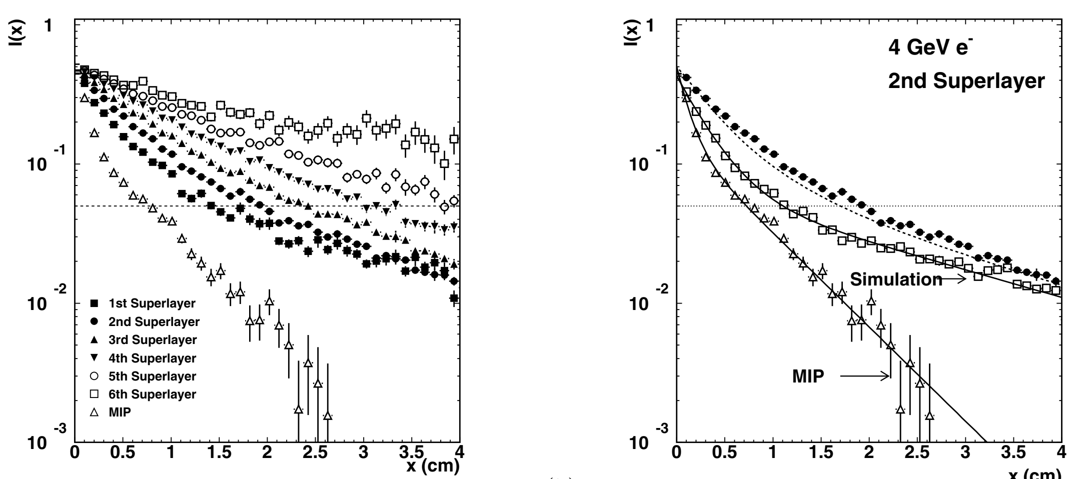

(a) (b)

Figure 3: (a) Integral lateral shower profiles at each superlayer for 4 GeV electrons and MIPs. (b) Comparison with the simulation at the second superlayer. Filled circles are data results and open squares are simulations. Dashed curve, which is a convolution of the MIP and the simulation, is consistent with beam data.

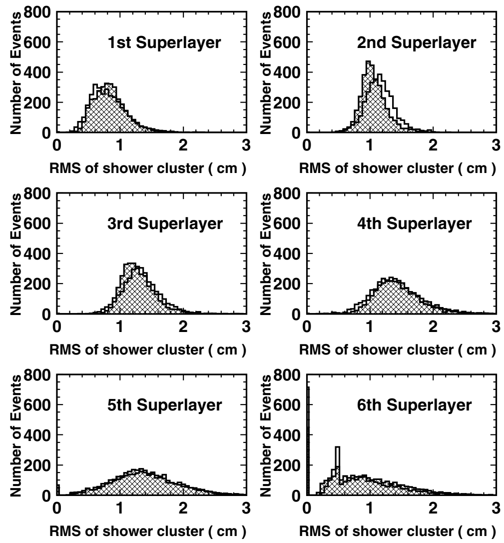

Figure 4: Root-mean-square distributions at each superlayer. Open histograms are testbeam results, and hatched are simulation results.

3. BASIC STUDIES OF GEANT4

3.1. Range Cuts

Before performing the full simulation with the detailed geometry, we try to do some basic validations with simple testbeam-like geometry, since we have not enough experience of using GEANT4.

First, we check dependence of the range cut in GEANT4 (6.2.p2) because it significantly affects the energy deposits in a sampling calorimeter which we are studying for the linear collider experiments.

Figure 5 shows the energy cuts as a function of the range cut for some materials which are often used in calorimeters, for (a) electrons and (b) photons. Large differences between the materials exist at 1 mm, which is the default value of the range cut. The total energy deposits in absorbers and active media are shown in Fig. 6 (a) and (b), respectively, for two sampling calorimeters: 2.5 mm tungsten + 1 mm scintillator, and 4 mm lead + 1 mm scintillator. In both configurations we see threshold behaviors around 0.3 μm $\sim$ 10 μm. Decomposing the physics effects in GEANT4, it turns out that the behaviors originates mainly from the multiple scatterings, which apparently have the mean-free-path around the region. Therefore, we have to choose a range cut value as small as $\sim 1\mu$m for GEANT4 simulation,

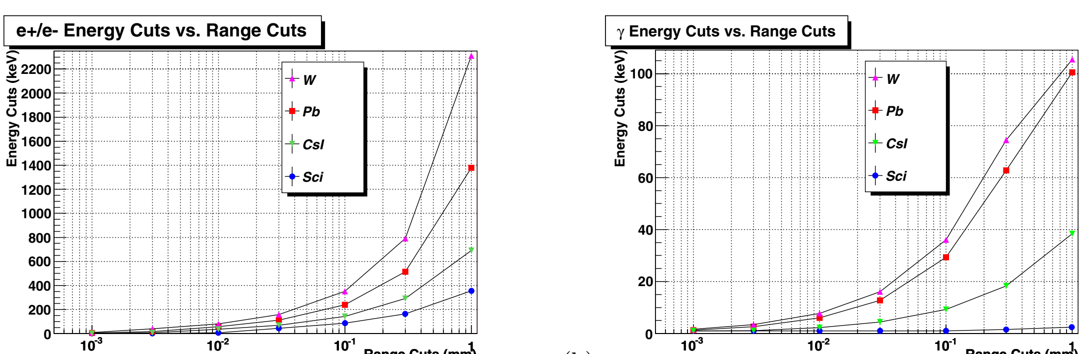

(a) (b)

Figure 5: Energy cuts vs. range cuts for (a) electrons and (b) photons.

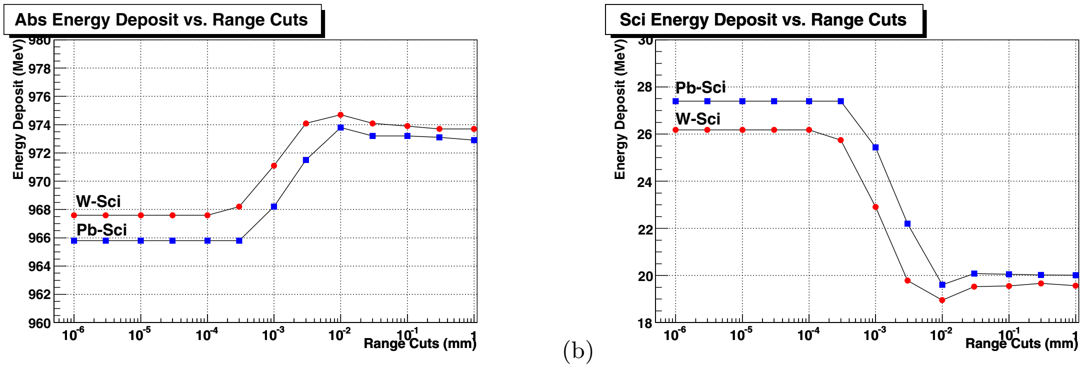

(a) (b)

Figure 6: Total energy deposits in (a) absorbers and (b) active media (scintillators).

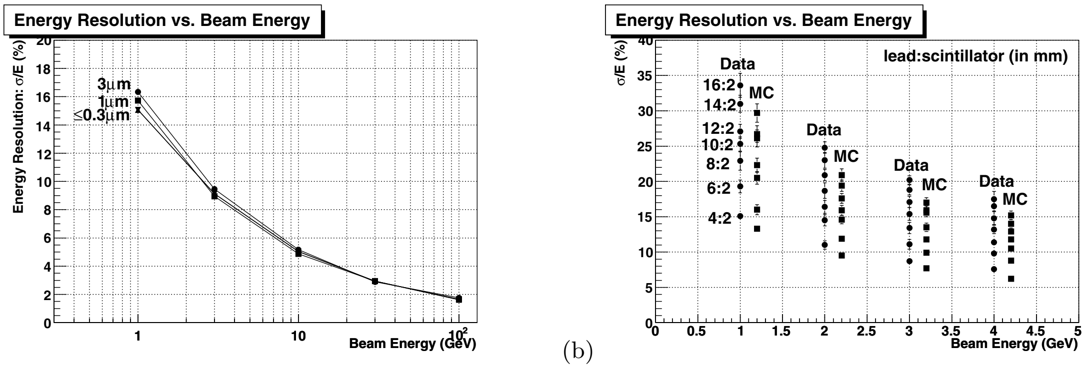

(a) (b)

Figure 7: Energy resolution vs. electron beam energy. (a) The range cut value is set to 0.3, 1 or 3μm. (b) Comparison with testbeam data for several sampling ratios.

but this should be optimized together with a parameter called maximum step-length to save CPU consumption.

3.2. Energy Resolution

Figure 7 (a) shows the energy resolutions for electrons measured with 4mm-lead/1mm-sci. sampling calorimeter Small discrepancies are seen at 1 GeV between the range cuts of 0.3, 1 and 3μm, but in all cases the reasonable energy resolutions of $\sim 16\%/\sqrt{E}$ are obtained.

Comparison with testbeam results [1] is also made for validation, as shown in Fig. 7 (b). Electrons are injected into the calorimeter, for which the lead/sci. sampling ratio is varied by changing the lead thickness. Because the MC simulation dose not include detector effects such as photo-statistics, MC results are slightly smaller than the data, but in general, EM shower is well simulated by GEANT4 with proper settings. We plan to do same validation for hadron showers.

References

[1] T. Suzuki et al, Nucl. Instr. Meth. A.432 (1999) 48; S. Uozumi et al, Nucl. Instr. Meth. A.487 (2002) 291.

[2] H. Matsunaga, Proc. of LCWS2002, p. 592, Jeju, Korea, August 2002; A. Nagano et al, Submitted to Nucl. Instr. Meth. A.